

Wideband Source Localization Using One-Bit Quantized Arrays

Ryan M. Corey and Andrew C. Singer
University of Illinois at Urbana-Champaign

Abstract—We consider the problem of source localization with signals that are quantized to a single bit. While this problem has been previously addressed for narrowband signals quantized in complex baseband, we consider wideband signals quantized directly in the time domain. We adapt the generalized cross correlation estimator to work with quantized signals and analyze its theoretical performance as a function of the signal-to-noise ratio (SNR). We find that quantization imposes a small penalty at low SNR but scales poorly at high SNR. Furthermore, we analyze the effects of sampling on estimation performance and show that oversampling is necessary at high SNR. Finally, we apply the generalized cross correlation weighting function to steered response power direction-of-arrival estimation with a larger array. We demonstrate the performance of the system for speech localization.

Keywords—DOA estimation, delay estimation, coarse quantization, source localization, array processing

I. INTRODUCTION

We often wish to discover the spatial location of a signal, such as a radio transmission or a sound source. Arrays of sensors, such as antennas or microphones, can be used to determine the direction of arrival (DOA) based on relative time delays between sensors. Here, we consider source localization from one-bit signals. Single-bit sensors, which require trivial analog-to-digital conversion hardware, have no constraints on input-output linearity, and use much less bandwidth than high-precision sensors, have recently attracted interest in wireless communication applications. Coarsely quantized arrays have been shown to suffer only modest communication throughput penalties [1], [2], [3] and have also been successfully used for channel estimation [4], [5], [6]. These inexpensive sensors are attractive for so-called “massive” arrays with many elements [7]. As a parameter estimation problem, source localization should be well suited to systems with low-resolution measurements.

The problem of localization from one-bit quantized signals has previously been considered in the narrowband case, for which time delays correspond to phase shifts at the carrier frequency [8], [9], [10]. These authors apply quantization separately to the real and imaginary components of a complex baseband representation. Narrowband signals exhibit peculiar behavior when quantized to a single bit; for example, performance depends strongly on the direction of arrival [8]. Other authors have considered intensity-based localization with coarse quantization [11]. Here, we consider wideband, real-valued signals, such as those encountered in acoustic localization problems. Because multichannel localization relies on the phase structure of the source signal, results for narrowband signals do not necessarily extend to the wideband case. In this work, we consider the achievable performance and scaling of one-bit DOA estimation. First, we adapt a commonly used wideband time delay estimation algorithm, known as generalized cross correlation, for one-bit signals. We use a statistical

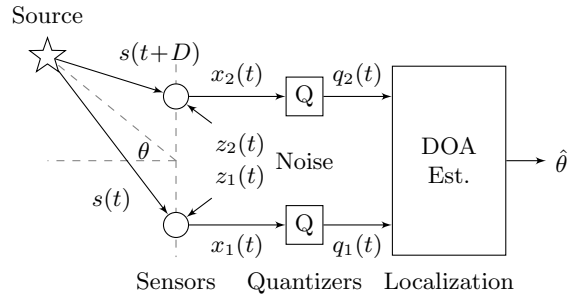


Fig. 1. Sources can be localized based on the signals’ time differences of arrival. We are interested in sensors that output one-bit quantized signals.

model of quantized noise to analyze its achievable performance. We then extend the results to multichannel DOA estimation and verify the system’s performance experimentally. The results suggest that wideband localization performance is relatively insensitive to single-bit quantization. Thus, it should be possible to build large arrays of single-bit sensors with high spatial diversity but low cost, bandwidth, and power.

II. CONTINUOUS-TIME DELAY ESTIMATION

A. Wideband TDOA estimation

The DOA θ of a faraway source can be deduced from the time differences of arrival (TDOA) between signals incident on the sensors of an array. Consider a source signal $s(t)$ and two sensors with additive noise signals $z_1(t)$ and $z_2(t)$, as shown in Figure 1. Assuming lossless isotropic propagation, the observed signals are

$$x_1(t) = s(t) + z_1(t) \quad (1)$$

$$x_2(t) = s(t + D) + z_2(t), \quad (2)$$

where D is the TDOA. To find the direction of the source, we must estimate D . If the source and noise signals are uncorrelated random processes, then the cross-correlation between $x_1(t)$ and $x_2(t)$ is

$$r_{x_1 x_2}(\tau) = \mathbb{E}[x_1(t)x_2(t - \tau)] \quad (3)$$

$$= r_s(\tau - D), \quad (4)$$

where $r_s(\tau - D)$ is the autocorrelation function of $s(t)$. Since the maximum of the autocorrelation occurs at zero lag, the maximum of $r_{x_1 x_2}(\tau)$ occurs at $\tau = D$. Thus, many methods of TDOA estimation aim to maximize an estimate of the cross-correlation of the observed signals. However, if the source signal is quasi-periodic, if the signal is subject to reverberation, or if the signal-to-noise ratio (SNR) varies significantly with frequency, then simple cross-correlation often performs poorly. Instead, we can choose from a class of generalized cross-correlation (GCC) estimators [12]:

$$\hat{D}_{\text{GCC}} = \arg \max_{\tau} \int_{-\infty}^{\infty} \psi(\Omega) \hat{R}_{x_1 x_2}(\Omega) e^{j\Omega\tau} d\Omega, \quad (5)$$

This work was supported in part by Systems on Nanoscale Information fabriCs (SONIC), one of the six SRC STARnet centers sponsored by MARCO and DARPA. This material is based upon work supported by the National Science Foundation Graduate Research Fellowship Program under Grant Number DGE-1144245.

where the estimated cross-power spectral density (PSD) $\hat{R}_{x_1, x_2}(\Omega)$ is the Fourier transform of the sample cross-correlation $\hat{r}_{x_1 x_2}(\tau)$ from a length- T observation of $x_1(t)$ and $x_2(t)$. The weighting function $\psi(\Omega)$ accounts for the source and noise spectra. There have been many proposed weighting functions [12], but we restrict our attention to the maximum likelihood estimator (GCC-ML).

First, suppose that the source and noise signals are stationary and Gaussian with known second-order statistics. Then the signal vector $\mathbf{x}(t) = [x_1(t), x_2(t)]^T$ has the cross-PSD matrix

$$R_{\mathbf{x}}(\Omega) = \begin{bmatrix} R_{x_1 x_1}(\Omega) & R_{x_1 x_2}(\Omega) \\ R_{x_2 x_1}(\Omega) & R_{x_2 x_2}(\Omega) \end{bmatrix}, \quad (6)$$

where $R_{x_1 x_2}(\Omega)$ and $R_{x_2 x_1}(\Omega)$ depend on D . Following the procedure of [12], for sufficiently long T we can model the log-likelihood of the observed signal as proportional to $\int_{-\infty}^{\infty} \mathbf{X}^*(\Omega) R_{\mathbf{x}}(\Omega) \mathbf{X}(\Omega) d\Omega$, where $\mathbf{X}(\Omega)$ is the continuous-time Fourier transform of the observed signal vector. Then the maximum likelihood estimator for D is given by (5) with weighting function

$$\psi_{\text{ML}}(\Omega) = \frac{1}{|R_{x_1 x_2}(\Omega)|} \frac{\gamma_x^2(\Omega)}{1 - \gamma_x^2(\Omega)}, \quad (7)$$

where

$$\gamma_x^2(\Omega) = |R_{x_1 x_2}(\Omega)|^2 / R_{x_1 x_1}(\Omega) R_{x_2 x_2}(\Omega) \quad (8)$$

depends on the signal-to-noise ratio (SNR). The GCC-ML estimator achieves the Cramér-Rao lower bound (CRLB) for Gaussian TDOA estimation, which is given by [12], [13]

$$\text{Var}(\hat{D}) \geq \left[\frac{T}{2\pi} \int_{-\infty}^{\infty} \Omega^2 \frac{\gamma_x^2(\Omega)}{1 - \gamma_x^2(\Omega)} d\Omega \right]^{-1}. \quad (9)$$

B. Quantized TDOA estimation

Now suppose that, due to restrictions on cost, power, speed, or bandwidth, each sensor produces only a one-bit representation of the signal. That is, each received signal $x_m(t)$ is quantized to

$$q_m(t) = \begin{cases} +1, & \text{if } x_m(t) \geq 0 \\ -1, & \text{if } x_m(t) < 0. \end{cases} \quad (10)$$

Note that $q_m(t)$ is a continuous-time signal with binary-valued amplitude. In the narrowband case, the likelihood function of the quantized complex baseband signal can be computed using orthant probabilities [8] or approximated using simpler distributions [10]. In the wideband case considered here, we will assume that the Fourier series coefficients of the quantized signals are Gaussian even though the time-domain signals are not, allowing us to apply the frequency-domain likelihood model of [12] for large T .

We first find the auto- and cross-correlation of the quantized inputs using the ‘‘arcsine law’’ [14], which states that for real Gaussian random variables A and B with zero mean and unit variance,

$$\mathbb{E}[\text{sign}(A)\text{sign}(B)] = \frac{2}{\pi} \arcsin(\mathbb{E}[AB]). \quad (11)$$

Suppose that $z_1(t)$ and $z_2(t)$ share the same autocorrelation $r_z(\tau)$ but are uncorrelated with each other and $s(t)$. By the arcsine law, the auto- and cross-correlations of $q_1(t)$ and $q_2(t)$ are

$$r_{q_1 q_1}(\tau) = \frac{2}{\pi} \arcsin\left(\frac{r_s(\tau) + r_z(\tau)}{r_s(0) + r_z(0)}\right) \quad (12)$$

$$r_{q_1 q_2}(\tau) = \frac{2}{\pi} \arcsin\left(\frac{r_s(\tau - D)}{r_s(0) + r_z(0)}\right), \quad (13)$$

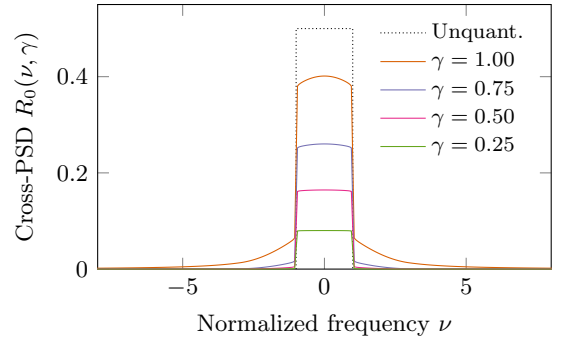


Fig. 2. The normalized cross-PSD of quantized bandlimited Gaussian signals at various SNRs. The dotted line shows the unquantized spectrum.

and similarly for $r_{q_2 q_2}$ and $r_{q_2 q_1}$. Note that, unlike in (4), the quantized cross-correlation depends on the noise power. The nonlinearity of the quantizer couples the signal and noise.

Next, assume that the sample interval T is sufficiently long that the frequency-domain Gaussian likelihood model applies. The entries of the cross-power spectral density matrix (6) are given by

$$R_{q_1 q_1}(\Omega) = \int_{-\infty}^{\infty} \frac{2}{\pi} \arcsin\left(\frac{r_s(\tau) + r_z(\tau)}{r_s(0) + r_z(0)}\right) e^{-j\Omega\tau} d\tau \quad (14)$$

$$R_{q_1 q_2}(\Omega) = e^{-j\Omega D} \int_{-\infty}^{\infty} \frac{2}{\pi} \arcsin\left(\frac{r_s(\tau)}{r_s(0) + r_z(0)}\right) e^{-j\Omega\tau} d\tau. \quad (15)$$

Since we have assumed that $z_1(t)$ and $z_2(t)$ have the same distribution, $R_{q_2 q_2}(\Omega) = R_{q_1 q_1}(\Omega)$. The quantized GCC-ML estimator can be found by substituting $R_{q_1 q_1}$, $R_{q_2 q_2}$, and $R_{q_1 q_2}$ for the corresponding variables in (7) and (8):

$$\hat{D}_{\text{Q-ML}} = \arg \max_{\tau} \int_{-\infty}^{\infty} \frac{\hat{R}_{q_1 q_2}(\Omega)}{|R_{q_1 q_2}(\Omega)|} \frac{\gamma_q^2(\Omega)}{1 - \gamma_q^2(\Omega)} e^{j\Omega\tau} d\Omega \quad (16)$$

$$\gamma_q^2(\Omega) = |R_{q_1 q_2}(\Omega)|^2 / R_{q_1 q_1}(\Omega). \quad (17)$$

The CRLB for estimating D from a finite-length observation of continuous-time quantized signals is then

$$\text{Var}(\hat{D}_{\text{Q}}) \geq \left[\frac{T}{2\pi} \int_{-\infty}^{\infty} \Omega^2 \frac{\gamma_q^2(\Omega)}{1 - \gamma_q^2(\Omega)} d\Omega \right]^{-1}. \quad (18)$$

C. Flat bandlimited noise

To assess the achievable performance of source localization with wideband signals, let us consider bandlimited Gaussian signals. Suppose that the source has constant PSD P_s on the interval $\Omega \in [-\Omega_0, \Omega_0]$ and zero elsewhere, and that the sensor noise has constant PSD P_z on that interval. Then $\gamma_x(\Omega) = P_s / (P_s + P_z)$ is constant on that interval and (9) reduces to

$$\text{Var}(\hat{D}) \geq \frac{3\pi}{T\Omega_0^3} \frac{1 - \gamma_x^2}{\gamma_x^2}. \quad (19)$$

Now let us analyze the achievable estimation performance for the one-bit quantized signal. Suppose that $z_1(t)$ and $z_2(t)$ are also bandlimited to $\Omega \in [-\Omega_0, \Omega_0]$. The autocorrelation functions are

$$r_s(\tau) = P_s \frac{\Omega_0}{\pi} \text{sinc}(\Omega_0 \tau) \quad (20)$$

$$r_z(\tau) = P_z \frac{\Omega_0}{\pi} \text{sinc}(\Omega_0 \tau), \quad (21)$$

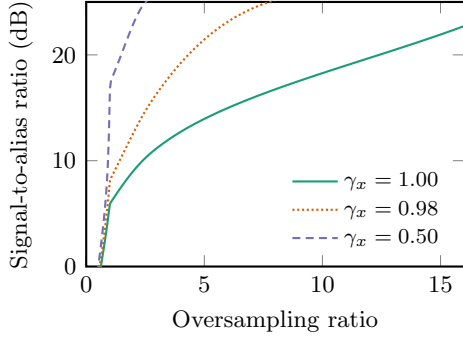


Fig. 3. Oversampling can significantly reduce the energy in aliasing artifacts, particularly at low to moderate SNR. Note the corner points at the Nyquist rate (OSR = 1).

where $\text{sinc}(u) = \sin(u)/u$ for $u \neq 0$ and 1 for $u = 0$. Placing these autocorrelations into (14) and (15) yields

$$R_{q_1 q_1}(\Omega) = \int_{-\infty}^{\infty} \frac{2}{\pi} \arcsin(\text{sinc}\Omega_0\tau) e^{-j\Omega\tau} d\tau \quad (22)$$

$$R_{q_1 q_2}(\Omega) = e^{-j\Omega D} \int_{-\infty}^{\infty} \frac{2}{\pi} \arcsin(\gamma_x \text{sinc}\Omega_0\tau) e^{-j\Omega\tau} d\tau. \quad (23)$$

Let us define the normalized spectral density function

$$R_0(\nu, \gamma) = \int_{-\infty}^{\infty} \frac{2}{\pi} \arcsin(\gamma \text{sinc}(2\pi\tau)) e^{-j2\pi\nu\tau} d\tau. \quad (24)$$

This function is shown in Figure 2 for several values of γ . For large γ , there is significant leakage outside the original signal band. For small γ , it approaches a rectangle with area $\frac{2}{\pi} \arcsin(\gamma)$. In this low-SNR regime, the out-of-band quantization artifacts are uncorrelated between the two sensors, so they have little impact on the cross-PSD at higher frequencies.

From (17), we find that

$$\gamma_q(\Omega) = R_0\left(\frac{\Omega}{\Omega_0}, \gamma_x\right) / R_0\left(\frac{\Omega}{\Omega_0}, 1\right). \quad (25)$$

At low SNR, $\gamma_q(\Omega) \approx \frac{2}{\pi} \arcsin(\gamma_x)$ for $\Omega \in [-\Omega_0, \Omega_0]$ and zero elsewhere, so the continuous-time quantized CRLB is approximately

$$\text{Var}(\hat{D}_Q) \geq \frac{3\pi}{T\Omega_0^3} \frac{1 - \left(\frac{2}{\pi} \arcsin \gamma_x\right)^2}{\left(\frac{2}{\pi} \arcsin \gamma_x\right)^2}, \quad \gamma_x \ll 1, \quad (26)$$

which is a factor of $\pi^2/4$ higher than for unquantized signals. This is equivalent to a $\pi/2$ (1.96 dB) reduction in SNR, which is consistent with previously reported results for narrowband TDOA estimation [9]. At high SNR, however, the variance bound of the quantized signal estimator decreases more slowly than that of the unquantized estimator. We will show in the next section that the CRLB is not particularly useful at high SNR because performance is limited by sampling rather than sensor noise.

III. DISCRETE-TIME DELAY ESTIMATION

The analysis above applies to continuous-time signals. However, practical localization systems must also sample the sensor inputs. Let Δ denote the sample period of the system. The sampled signals are

$$x_1[n] = x_1(n\Delta) \quad (27)$$

$$x_2[n] = x_2(n\Delta). \quad (28)$$

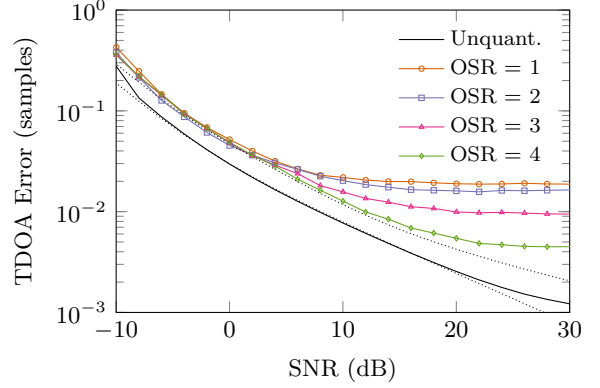


Fig. 4. Standard deviation of the delay estimate for bandlimited Gaussian source and noise signals with various oversampling ratios. The dotted curves are the unquantized and quantized continuous-time CRLBs. Here $D = -3.20$ samples.

In the unquantized case, it is sufficient to sample at the Nyquist rate, $\Delta = \pi/\Omega_0$ for our bandlimited noise example. However, quantization generates out-of-band artifacts that can alias into the signal band. At low SNR, these artifacts are uncorrelated between sensors and do not affect the cross-correlation, but at high SNR they are the dominant source of error.

For the bandlimited Gaussian signals of Section II-C, we can use the quantized spectrum to compute the power in the aliased artifacts as a function of the oversampling ratio (OSR) and γ_x :

$$2 \int_{\frac{\pi}{\Delta}}^{\infty} |R_{q_1 q_2}(\Omega)| d\Omega = 2 \int_{\frac{\pi}{\Delta}}^{\infty} \frac{2\pi}{\Omega_0} R_0\left(\frac{\Omega}{\Omega_0}, \gamma_x\right) d\Omega \quad (29)$$

$$= 2 \int_{\text{OSR}}^{\infty} R_0(\nu, \gamma_x) d\nu. \quad (30)$$

Figure 3 shows the signal-to-aliasing power ratio for several values of γ_x . Sampling at the original Nyquist rate captures 81 percent of the total energy, for a signal-to-aliasing ratio of 6 dB. Oversampling by a factor of 16 gives a ratio of 23 dB.

It should be noted that the spectral energy ratio alone does not predict the performance of the estimator for a particular sample rate: it also depends on D . To see why, consider the discrete-time cross-PSD of the sampled and quantized signals:

$$\text{DTFT}\{r_{q_1 q_2}\} = \frac{1}{\Delta} \sum_{k=-\infty}^{\infty} R_{q_1 q_2} \left(\frac{\omega + 2\pi k}{\Delta} \right) \quad (31)$$

$$= \frac{1}{\Delta} \sum_{k=-\infty}^{\infty} \left| R_{q_1 q_2} \left(\frac{\omega + 2\pi k}{\Delta} \right) \right| e^{-j\frac{\omega + 2\pi k}{\Delta} D} \quad (32)$$

$$= \frac{1}{\Delta} e^{-j\frac{\omega D}{\Delta}} \sum_{k=-\infty}^{\infty} \left| R_{q_1 q_2} \left(\frac{\omega + 2\pi k}{\Delta} \right) \right| e^{-j\frac{2\pi k D}{\Delta}}. \quad (33)$$

If the delay is an integer multiple of Δ , then the aliased artifacts will have the same phase as the source signal; that is, the discrete-time cross-PSD will be $e^{-j\omega D/\Delta}$ times a sum of positive numbers. For most delay values, however, the terms in the sum for $k \neq 0$ will have arbitrary phases and distort the phase of the discrete-time cross-correlation.

Figure 4 shows the experimental performance compared to the continuous-time CRLB for the bandlimited Gaussian signals consid-

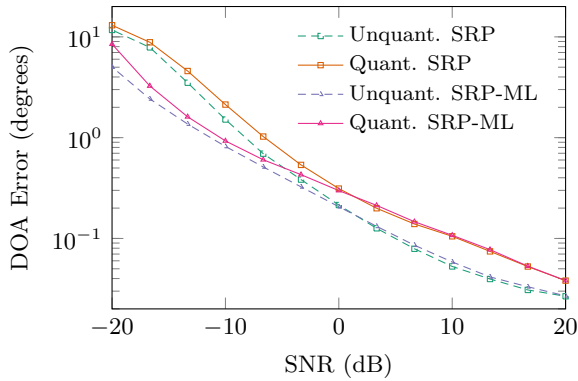


Fig. 5. Standard deviation of the DOA estimate as a function of SNR for a uniform linear array with different source and noise spectra.

ered in Section II-C. Aliasing noise creates a floor in the estimator performance at high SNR. If we wish to benefit from the low resource costs of one-bit sampling, then we must pay a penalty in the form of a higher sample rate.

IV. DIRECTION OF ARRIVAL ESTIMATION

A. Weighted steered response power

To accurately estimate the DOA of a source, we need more than just two sensors. Indeed, inexpensive one-bit sensors are best used in large numbers. The generalized cross correlation can be extended to more than two sensors using a weighted steered response power (SRP) beamformer [15], [16]. For a weighted delay-and-sum beamformer with M sensors and relative time differences $D_m(\theta)$ for $m = 1, \dots, M$, the output power is proportional to

$$P(\theta) = \int_{-\infty}^{\infty} \left| \sum_m \sqrt{\psi(\Omega)} X_m(\Omega) e^{j\Omega D_m(\theta)} \right|^2 d\Omega \quad (34)$$

$$= \int_{-\infty}^{\infty} \sum_m \sum_n \psi(\Omega) X_m(\Omega) X_n^*(\Omega) e^{j\Omega D_{mn}(\theta)} d\Omega, \quad (35)$$

where $D_{mn}(\theta) = D_m(\theta) - D_n(\theta)$ are the time differences of arrival. Thus, the SRP is simply the sum of the GCC powers for all sensor pairs. For a one-bit array, we can use the ML weights derived for the GCC to compute the SRP:

$$\hat{\theta}_{\text{ML}} = \arg \max_{\theta} \int_{-\infty}^{\infty} \frac{\gamma_q^2(\Omega)}{1 - \gamma_q^2(\Omega)} \frac{\left| \sum_m Q_m(\Omega) e^{j\Omega D_m(\theta)} \right|^2}{|R_{q_1 q_2}(\Omega)|} d\Omega. \quad (36)$$

B. Out-of-band noise

Unlike the simple delay-and-sum estimator, the maximum likelihood SRP (SRP-ML) estimator accounts for variations in SNR across frequency. Figure 5 shows quantized and unquantized localization performance as a function of SNR for two signals with different spectra: the target source is a speech-shaped (low-frequency) Gaussian signal, while the additive sensor noise is high-frequency Gaussian noise. The source is 45 degrees from broadside of a uniform linear array with eight ideal isotropic elements spaced 8 cm apart in far-field, anechoic conditions. Localization was performed on 100 ms blocks and the DOA estimation error was averaged over 50 blocks. The figure shows that the maximum likelihood estimator outperforms the conventional SRP estimator at low SNR.

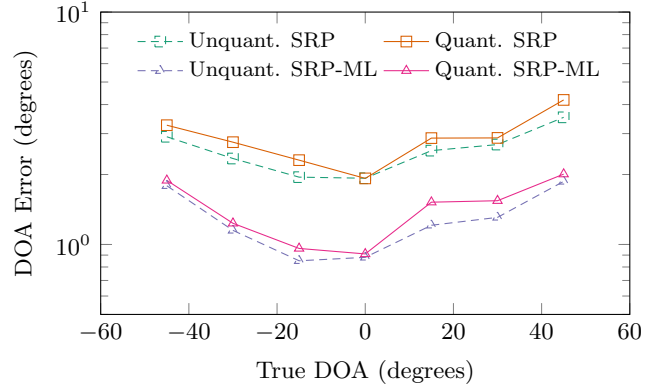


Fig. 6. Standard deviation of the DOA estimate as a function of angle of arrival for a linear array with a speech babble source and Gaussian noise.

C. Speech localization performance

To show the real-world performance of the quantized array, we conducted a speech localization experiment using a database of recorded impulse responses [17] from a uniform linear array with 8 cm spacing and a room reverberation time of 160 ms. The source signal is a speech babble mixture from ten talkers in the TIMIT database [18] and the noise is white Gaussian noise at -10 dB SNR. The DOA was estimated for overlapping blocks of length 26 ms and the results were averaged over 150 blocks. Figure 6 shows the performance of the array as a function of angle. The quantized array standard deviation is roughly 20 percent higher than that of the unquantized array for both estimators. The ML estimator, which was computed using a long-term average speech spectrum, has standard deviation roughly half that of the conventional SRP estimator for both quantized and unquantized signals.

It has been observed that narrowband quantized localization is sensitive to the angle of arrival: performance improves dramatically when the TDOA aligns with one fourth of the wavelength [8]. Here, while the performance varies as a function of angle, it does so for both the quantized and unquantized cases. With the exception of the sample rate sensitivity mentioned above, quantized wideband signals do not appear to exhibit such angle-sensitive behavior.

V. CONCLUSIONS

The theoretical results of Section II and the experiments of Section IV suggest that single-bit quantization has only a modest impact on source localization performance for wideband sources. At low SNR, where sensor noise is the limiting factor, binary quantization causes a familiar 1.96 dB penalty. At high SNR, where quantization error dominates, we must oversample to avoid performance degradation. Even so, single-bit sensors likely use much less power and bandwidth than high-precision sensors. Furthermore, the well-established GCC and SRP wideband localization methods can be easily adapted to work with coarsely quantized arrays. For source localization applications, therefore, it appears advantageous to build large arrays of single-bit sensors rather than smaller arrays of high-precision sensors.

REFERENCES

- [1] A. Mezghani and J. A. Nosse, "On ultra-wideband MIMO systems with 1-bit quantized outputs: Performance analysis and input optimization," in *Proceedings of the IEEE International Symposium on Information Theory (ISIT)*, pp. 1286–1289, 2007.

- [2] J. Singh, O. Dabeer, and U. Madhow, "On the limits of communication with low-precision analog-to-digital conversion at the receiver," *IEEE Transactions on Communications*, vol. 57, no. 12, 2009.
- [3] J. Mo and R. W. Heath, "Capacity analysis of one-bit quantized MIMO systems with transmitter channel state information," *IEEE Transactions on Signal Processing*, vol. 63, no. 20, pp. 5498–5512, 2015.
- [4] M. T. Ivrlac and J. A. Nosssek, "On MIMO channel estimation with single-bit signal-quantization," in *ITG Smart Antenna Workshop*, 2007.
- [5] G. Zeitler, G. Kramer, and A. Singer, "Bayesian parameter estimation using single-bit dithered quantization," *IEEE Transactions on Signal Processing*, vol. 60, pp. 2713–2726, June 2012.
- [6] J. Mo, P. Schniter, N. Gonzalez Prelcic, and R. Heath, "Channel estimation in millimeter wave MIMO systems with one-bit quantization," in *Asilomar Conference on Signals, Systems, and Computers*, pp. 957–961, 2014.
- [7] S. Jacobsson, G. Durisi, M. Coldrey, U. Gustavsson, and C. Studer, "One-bit massive MIMO: Channel estimation and high-order modulations," in *IEEE International Conference on Communication Workshop (ICCW)*, pp. 1304–1309, 2015.
- [8] O. Bar-Shalom and A. Weiss, "DOA estimation using one-bit quantized measurements," *IEEE Transactions on Aerospace and Electronic Systems*, vol. 38, no. 3, pp. 868–884, 2002.
- [9] M. Stein, A. Mezghani, and J. A. Nosssek, "Quantization-loss analysis for array signal-source localization," in *International ITG Workshop on Smart Antennas (WSA)*, pp. 1–8, VDE, 2013.
- [10] M. Stein, K. Barbé, and J. A. Nosssek, "DOA parameter estimation with 1-bit quantization bounds, methods and the exponential replacement," in *International ITG Workshop on Smart Antennas (WSA)*, pp. 1–6, VDE, 2016.
- [11] R. Niu and P. K. Varshney, "Target location estimation in sensor networks with quantized data," *IEEE Transactions on Signal Processing*, vol. 54, no. 12, pp. 4519–4528, 2006.
- [12] C. Knapp and G. Carter, "The generalized correlation method for estimation of time delay," *IEEE Transactions on Acoustics, Speech, and Signal Processing*, vol. 24, no. 4, pp. 320–327, 1976.
- [13] B. Friedlander, "On the cramer-rao bound for time delay and doppler estimation," *IEEE Transactions on Information Theory*, vol. 30, no. 3, pp. 575–580, 1984.
- [14] J. H. Van Vleck and D. Middleton, "The spectrum of clipped noise," *Proceedings of the IEEE*, vol. 54, no. 1, pp. 2–19, 1966.
- [15] M. S. Brandstein and H. F. Silverman, "A robust method for speech signal time-delay estimation in reverberant rooms," in *IEEE International Conference on Acoustics, Speech, and Signal Processing*, vol. 1, pp. 375–378, IEEE, 1997.
- [16] J. H. DiBiase, H. F. Silverman, and M. S. Brandstein, "Robust localization in reverberant rooms," in *Microphone Arrays*, pp. 157–180, Springer, 2001.
- [17] E. Hadad, F. Heese, P. Vary, and S. Gannot, "Multichannel audio database in various acoustic environments," in *International Workshop on Acoustic Signal Enhancement (IWAENC)*, pp. 313–317, IEEE, 2014.
- [18] J. S. Garofolo, L. F. Lamel, W. M. Fisher, J. G. Fiscus, and D. S. Pallett, "TIMIT acoustic-phonetic continuous speech corpus LDC93S1." Web Download, 1993.